

https://doi.org/10.1070/QEL16940

Evaluation of oxygenation in the surface layers of biological tissues based on diffuse optical spectroscopy with automated calibration of measurements

M.S. Kleshnin, I.V. Turchin

Abstract. **To assess the oxygen saturation (oxygenation) in the surface layers of biological tissues (at a depth of 4 mm), a compact system based on diffuse optical spectroscopy (DOS) with reflective measurement geometry in the wavelength range of 520–590 nm is proposed. The experimental DOS device is based on a broadband LED source of probe radiation and a spectrometer using a fibre-optic radiation delivery system. To calculate the oxygenation, an original method is proposed based on measuring the intensity of scattered light at four different locations of the source and receiver on the surface of the object under study (four-measurement method). The developed method allows for the device hardware parameters (optical contact with the tissue, transient characteristics of the radiation delivery system) and does not require any additional calibration measurements. The results of testing the DOS system using the four-measurement method for monitoring the oxygen saturation of tissues during the artificial occlusion of the blood vessels agree with the published data of other research teams.**

Keywords: *diffuse optical spectroscopy, oxygen saturation, optics of biological tissues, automation of measurements.*

1. Introduction

To date, it has already been proven that the course of many diseases (tumour processes [1, 2], diabetes mellitus [3, 4], as well as recovery after angiosurgery and plastic surgery [5, 6]) is largely dependent on the efficiency of delivery and utilisation of oxygen. Therefore, the task of timely diagnosis of oxygen saturation of tissues is one of the most important in modern medicine. The traditional approach to the assessment of oxygen saturation (oxygenation) of biological tissues is the polarographic measurement of the partial pressure of oxygen [7], but this is an invasive and lengthy procedure. A highly efficient method of non-invasive observation of tissue oxygenation is positron emission tomography [8], but this is a very expensive and technically complex technique. Currently, diffuse optical spectroscopy (DOS) [9–16] is being actively developed to study the oxygen saturation of tissues, which combines non-invasiveness and relatively low cost.

The DOS method is based on the calculation of the main indicators (absorption and transport scattering coefficients), which determine the propagation of multiply scattered light, by measuring the spectral intensity of the probe radiation transmitted through the object under study [9, 10]. This method can be used to determine the oxygen saturation of the tissue by the ratio of the partial absorption contributions of oxygenated and deoxygenated haemoglobin to the total absorption rate of the object under study [11, 17]. Therefore, the correct solution of the inverse problem is the key problem of the DOS.

Currently, there are several effective approaches to solving the inverse problem of DOS. For example, the use of amplitude-modulated [12, 13] or pulsed [13, 14] probe radiation allows separating absorption and transport scattering by the time parameters of the recorded signal (phase shift or pulse shape) at a fixed distance between the source and the light receiver. However, for studies of local tissue oxygenation in a small volume (100–1000 mm^3), i.e., at small (less than 1 cm) distances between the source and receiver, the use of these approaches is not justified, since in the case of modulated probe radiation, the phase shifts of photon density waves will be significant only at a very high modulation frequency exceeding 1 GHz, and in the case of pulsed radiation, the broadening of the probe pulse will not exceed 200 ps. Thus, in both above cases, the hardware implementation of the DOS system will be difficult and expensive. Therefore, to assess the oxygenation in the surface layer of the tissue, it is advisable to use cw probe radiation, but with several measurements at different distances between the source and the light receiver [15, 16]. At the same time, the information content can be significantly increased by using broadband sources of probe radiation and spectrometers, which will make it possible to distinguish between a large number of chromophores. In addition, the use of reflective measurement geometry makes it possible to evaluate the local oxygenation of surface tissue sites, regardless of the thickness of the object under study. Unfortunately, in this case, the problem of separating absorption and transport scattering no longer has an analytical solution; therefore, numerical methods should be used to calculate the oxygenation [18].

One of the main difficulties of the technical implementation of the DOS is the calibration of measurements, i.e., allowing for the hardware parameters involved in acquiring the experimental data (the background illumination, the shape of the light source spectrum, the gain of the receiving path, the transient characteristics of the radiation delivery system, the variations in optical contact with the tissue). As a rule, for preliminary calibration of DOS systems, testing on a standard (phantom with known scattering and absorbing properties close to the parameters of the tissues) is used. However, this procedure takes time and does not allow for changes in hardware parameters during the study, for example, due to heat-

M.S. Kleshnin, I.V. Turchin Institute of Applied Physics, Russian Academy of Sciences, ul. Ul'yanova 46, 603950 Nizhny Novgorod, Russia; e-mail: m.s.kleshnin@gmail.com, ilya@ufp.appl.sci-nnov.ru

Received 23 December 2018; revision received 28 January 2019
Kvantovaya Elektronika **49** (7) 628–632 (2019)
Translated by V.L. Derbov

ing, fibre curvature, contamination of an optical fibre or an object, etc.

This paper proposes an original four-measurement method based on detecting diffusely scattered light at four different spatial positions of the source and receiver on the surface of the object. This approach allows one to take into account the device hardware parameters during the measurements automatically and does not require any additional calibration procedure. To implement it, an DOS system has been constructed using a broadband LED source of probe radiation and a spectrometer. The device is equipped with a probe consisting of four fibres, the output ends of which are located on one straight line at equal distances from each other. For measurements, the fibre probe is brought into direct contact with the biological tissue. To assess the accuracy of the oxygenation calculation by means of the developed approach, numerical simulation of spectroscopic measurements is used. Testing of the developed DOS system was carried out on real biological objects in vivo.

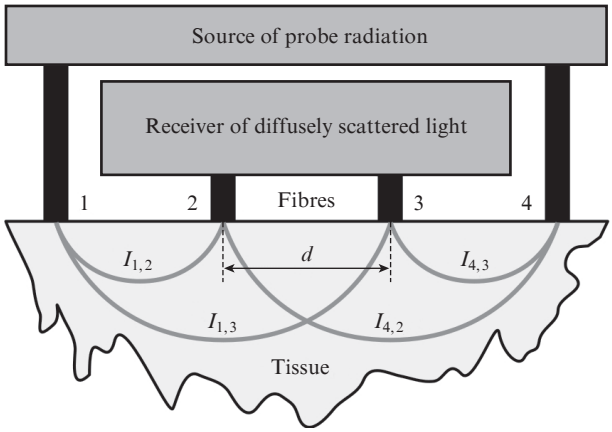

Figure 1. Schematic of the four-measurement method ($I_{S,R}$ is the recorded intensity of diffusely scattered light when the source is connected to the fibre S, and the receiver to the fibre R).

2. Materials and methods

2.1. Calculation of oxygen saturation based on spectroscopic measurements

The propagation of optical radiation in biological tissues is described with high precision by the diffusion approximation of the radiation transfer equation (RTE) [19], which has an analytical solution for the intensity I of diffusely scattered light in a homogeneous, unlimited turbid medium [19,20]:

$$I = I_0 \frac{\mu_a + \mu_s'}{r} \exp[-\sqrt{3\mu_a(\mu_a + \mu_s')}\, r], \quad (1)$$

where μ_a and μ_s' are the indices of absorption and transport scattering of light; r is the distance to a point source of probe radiation with an intensity I_0. With the hardware parameters of the DOS device with a fibre radiation delivery system for reflective measurement geometry taken into account, this expression takes the form

$$I = A_S A_R I_0 \frac{\mu_a + \mu_s'}{d_{S,R}} \exp\left[-\sqrt{3\mu_a(\mu_a + \mu_s')}\, d_{S,R}\right]. \quad (2)$$

Here $d_{S,R}$ is the distance between the output ends of the fibres from the source and the radiation receiver; and A_S and A_R are the transient characteristics of the DOS device parts from the source of the probe radiation to the object under study and from the object to the receiver of diffusely scattered light, respectively. The transient characteristics depend on factors such as the quality of the optical contact of the fibres with the object, as well as on the loss and repeated reflection in the fibres; therefore, they are difficult to allow for, when calibrating the DOS device with a reference phantom.

In the present work, to take into account the transient characteristics of the DOS system, it is proposed to use a special measurement geometry presented in Fig. 1. The idea of the proposed approach is to use a four-fibre probe with a fixed distance d between adjacent exits. In this case, each of the fibres can be connected to a source of probe radiation or a receiver of diffusely scattered light; therefore, the indices S and R in Eqn (2) will correspond to the numbers of the fibres connected to the source and receiver. Thus, if measurements are made when the source is connected successively to fibres 1 and 4, and the receiver to fibres 2 and 3, then a linear combination of the experimental data obtained will allow elimination of the hardware parameters from Eqn (2) and reduce it to the form:

$$2\exp[\sqrt{3\mu_a(\mu_a + \mu_s')}\, d] = \sqrt{\frac{I_{1,2}I_{4,3}}{I_{1,3}I_{4,2}}}. \quad (3)$$

To calculate the oxygenation StO_2 using Eqn (3), it is convenient to use the standard approximation of the transport scattering coefficient by a power function of the wavelength λ. The absorption coefficient is represented by a weighted sum of the absorption indices of the components of the object under study [20, 21]:

$$\mu_s' = \beta\left[\frac{\lambda_0}{\lambda}\right]^{\alpha}, \quad \mu_a = (1 - \mathrm{THb})\,\mu_a^{\mathrm{oth}}(\lambda)$$

$$+ \mathrm{THb}[\mathrm{StO_2}\,\mu_a^{\mathrm{HbO}}(\lambda) + (1 - \mathrm{StO_2})\,\mu_a^{\mathrm{HHb}}(\lambda)], \quad (4)$$

where THb is the total haemoglobin fraction in the chromophores of the studied object; α, β, λ_0 are the approximation coefficients of the transport scattering index; μ_a^{HbO}, μ_a^{HHb} are the normalised tabular absorption indices of the oxygenated and deoxygenated haemoglobin; and μ_a^{oth} is the total absorption rate of the remaining chromophores (water, lipids, melanin) (Fig. 2) [22]. Then the oxygen saturation of the tissue is determined by the numerical solution of the optimisation problem:

$$\sum_{\lambda}\left[\sqrt{\frac{I_{1,2}I_{4,3}}{I_{1,3}I_{4,2}}} - 2\exp[\sqrt{3\mu_a(\mu_a + \mu_s')}\, d]\right]^2_{\mathrm{THb,StO_2},\alpha,\beta} \to \min. \quad (5)$$

In this case, the coefficient β in Eqn (4) should ensure only the fulfilment of the diffusion approximation condition for the radiation transfer equation (RTE) $\mu_a \ll \mu_s'$, and its value can be almost arbitrary, since it has little effect on the result of the calculation of oxygenation compared to random measurement errors [23]. In addition, Fig. 2 shows that the effect of light absorption by water molecules in the wavelength range of 520–590 nm is very small, and the weighted sum of the absorption of fat and melanin is a monotonically decreasing function of the wavelength, as is the transport light scattering index [see Eqn (4)]. The only non-monotonic curve is the abs-

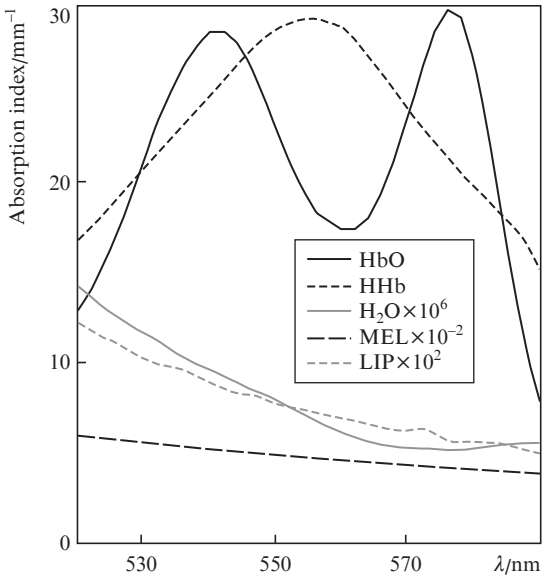

Figure 2. Absorption spectra of light for the main chromophores of biological tissue: water (H_2O), fat (LIP), melanin (MEL), oxyhaemoglobin (HbO) and deoxyhaemoglobin (HHb).

orption spectrum of haemoglobin. Thus, to calculate the oxygen saturation of the tissue, it is necessary to select only the non-monotonic component of the recorded data, and it no longer makes sense to separate the two remaining monotonic curves. Therefore, it is possible not to take into account the shape of the absorption spectrum of all the chromophores except the haemoglobin components, assuming $\mu_a^{oth}(\lambda) \approx 1$.

The function of the mean square error in the optimisation problem of the DOS (5) is twice differentiable; accordingly, to calculate the oxygen saturation, one can use the iterative algorithms of the first (gradient descent, Levenberg–Marquardt method) and second (Newton method, Broyden–Fletcher–Goldfarb–Shanno method) order [24]. However, second-order methods are very laborious (using the second derivatives of the error function) and are as efficient as possible only near the expected minimum, therefore, in this work, the standard Levenberg–Marquardt algorithm was used to solve the inverse DOS problem.

2.2. DOS system for assessing the oxygen saturation of biological tissues

For the technical implementation of the developed four-measurement method, an experimental DOS system was designed to estimate the oxygen saturation of the surface layers of biological tissues. Figure 3 presents a schematic of the proposed device, the design of which is based on using a broadband source of probe radiation (MCWHF2 from Thorlabs Inc., USA) and a QE65000 spectrometer (Ocean Optics Inc., USA). A probe consisting of silica fibres (Polironik LLC, Russia) 250 μm in diameter with a fixed spacing of 2 mm between adjacent exits was used to study biological tissues. In this case, the probe inputs are connected to the outputs of the source and the radiation receiver via an F-104-03 optical switch (Piezosystem Jena, GmbH). To control the force of pressing the contact surface of the probe to the object of study, a mechanical dynamometer was used. The DOS system is fully automated using Java 1.8 software (Oracle Co., USA).

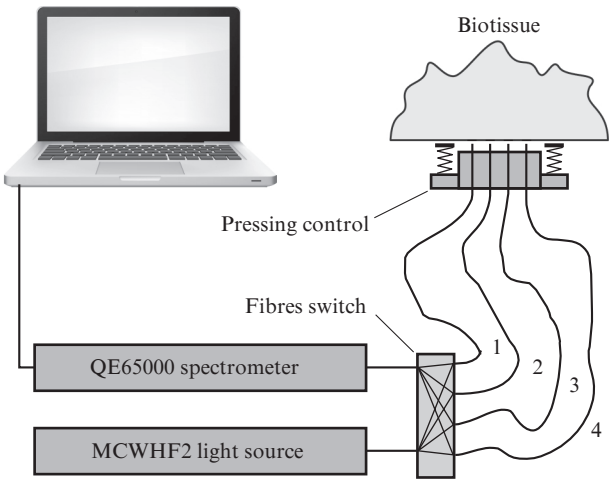

Figure 3. Schematic of the DOS system for assessing the oxygen saturation of biological tissues using the reflective geometry of spectroscopic measurements.

2.3. Estimation of the depth of the biological tissues probing

The average depth of the study of biological tissues h for the developed DOS system can be determined using the standard equation of 'banana-like' light paths in the tissue from the source to the receiver [25]:

$$h = \frac{r_{S,R}^{max}}{2\sqrt{2}}, \quad (6)$$

where $r_{S,R}^{max}$ is the maximum distance between the source and receiver in the course of measurements, which is 6 mm when the source is connected successively to fibres 1 and 2, and the receiver to fibres 3 and 4. However, this estimate gives the maximum depth for the most probable trajectory of photons, whereas the scatter of path data may be comparable with this value and the actual depth of probing will be greater.

In this work, the depth of biotissue probing is determined by the position of the photon trajectory along which a tenfold decrease in the intensity of probe radiation occurs as compared to that along the shortest path at the maximum distance between the source and the receiver:

$$\varepsilon \exp[-3\sqrt{3\mu_a(\mu_a+\mu_s')}\,d] = 10\exp[-3\varepsilon\sqrt{3\mu_a(\mu_a+\mu_s')}\,d]. \quad (7)$$

Then $h = 1.5\sqrt{\varepsilon^2 - 1}$. Thus, the depth of biological tissue probing is determined by the parameter ε, which depends on the optical properties of the particular sample under study and can vary from 1.44 to 2.78 (experimentally observed values), which corresponds to $h = 2$–4 mm.

2.4. Evaluation of the accuracy of calculating the tissue oxygen saturation

To assess the accuracy of the developed four-measurement method, we used statistical analysis of the error in the calculation of oxygenation from the results of numerical simulation of spectroscopic measurements. The measurements were simulated using the RTE in diffusion approximation, taking into account the boundary conditions [26], and adding noise simulating random errors in the experimental data:

$$I = I_0 \frac{\mu_s'}{\mu_t'}\left[\frac{\rho_1^{-2}}{\mu_t'}\left(\mu_E + \frac{1}{\rho_1}\right)\exp[-\mu_E\rho_1] + \frac{1}{\rho_2^2}\left(\frac{1}{\mu_t'} + 2z_b\right)\right.$$
$$\left.\times\left(\mu_E + \frac{1}{\rho_2}\right)\exp[-\mu_E\rho_2]\right] + \delta N;$$

$$\rho_1 = \sqrt{r^2 + \mu_t'^{-2}};\ \ \rho_2 = \sqrt{r^2 + (\mu_t'^{-1} + 2z_b)^2}; \qquad (8)$$

$$z_b = \frac{1(1+k)}{3\mu_t'(1-k)};\ \ \mu_E = \sqrt{3\mu_a\mu_t'};$$

$$\mu_t' = \mu_a + \mu_s';\ k = 0.67 - 1.44n^{-2} + 0.71n^{-1} + 0.66n;\ n = 1.4.$$

Here n is the refractive index; z_b is the extrapolated Milne length; N is a random variable with uniform distribution in the segment $[-\max(I), \max(I)]$; and δ is the noise level. The absorption spectrum of all biological chromophores except the haemoglobin components was approximated by a monotonically decreasing function:

$$\mu_a^{oth}(\lambda) = 1 - p\left[\frac{\lambda - 520}{70}\right]^q, \qquad (9)$$

in which q is a random variable with a uniform distribution in the interval [0.5, 1], and p is a variable parameter determining the relative change of the spectrum in the range of 520–590 nm.

The average absolute error in the calculation of oxygen saturation and its 95% confidence interval were calculated for 5000 spectroscopic measurements of biological tissues with random component composition. The fulfilment of the central limit theorem [27, 28], and the normality of the sample was checked by the formal Shapiro–Wilk test [28]. To assess the significance of the results obtained, Student's and Wilcoxon's tests were used [27, 29]. The modelling of spectroscopic measurements and the implementation of statistical analysis of the data obtained were performed using the Python 3.6 software environment.

2.5. Testing the DOS system on biological tissues

To test the developed DOS system on biological tissues in vivo, a series of experiments on occlusion modelling [30, 31] were performed on the fingers of a volunteer from the group of authors of the paper. Spectroscopic measurements and calculation of the oxygen saturation of the tissue were carried out before, during, and after the artificial occlusion of blood vessels. To limit the blood flow, a rubber band was applied to the base of the finger.

3. Results and discussion

Figure 4a shows the dependence of the average absolute error of the calculation of tissue oxygenation on the level of random noise in the experimental data. It is seen that an increase in the random noise level leads to an increase in the computational error, but its value is comparable to the noise level and becomes smaller when the noise exceeds 5%. In addition, if the proportion of haemoglobin absorption in a tissue sample is at least 10%, then the error in the calculation of oxygenation decreases by more than 1.5 times. At the same time, neglecting the monotonic component of the absorption spectrum leads to a significant calculation error only if the relative change of this component exceeds 40%, whereas the relative change in the intensity of the absorption spectrum of melanin in the range of 520–590 nm is 36%, and the absorption by fat is significantly (by 1000 times) smaller than that by melanin. When the proportion of haemoglobin absorption in the tissue exceeds 30%, the error in the calculation of oxygenation will be less than 2%.

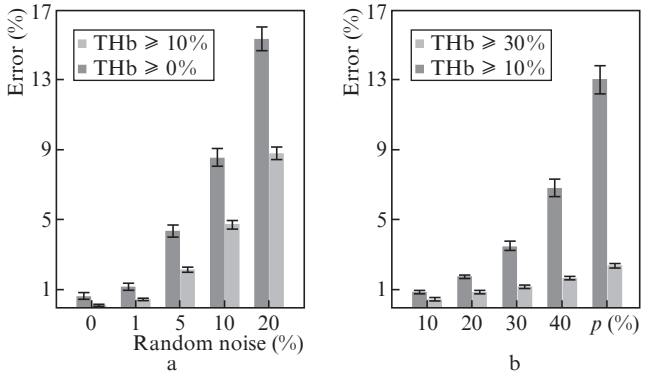

Figure 4. Average absolute error of the calculation of the biotissue oxygen saturation (a) for different levels of random noise in the experimental data and (b) various relative changes in the absorption spectrum of unaccounted chromophores while limiting the minimum fraction of haemoglobin.

The presented results are statistically significant at a level of less than 10^{-20} according to Student and Wilcoxon, and so it can be assumed that in the study of real biological tissues the error in the calculation of oxygenation will not exceed the error of spectroscopic measurements. Based on the obtained values of the error in calculating oxygenation at a low noise level, we also note that taking into account the boundary conditions in the proposed four-measurement method can increase the accuracy of calculations by no more than 1%. This is usually below the level of observed noise in the experimental data. This conclusion can also be extrapolated to evaluate the effect of the flat-layered structure of the object under study on the computational error, i.e., if the tissue oxygenation is the same in all layers, then the error in the calculation of oxygen saturation should not exceed 1%, since the influence of the air–tissue boundary is much more significant than the effect of weak changes in the optical properties between the layers. However, if each layer has its own oxygenation, it is impossible to calculate their values and estimate the calculation error, since it is not clear how to determine it. It is also important to note that all the assertions about the magnitude of the calculation error are valid only for calculating the oxygen saturation of the tissues using the four-measurement method in the 520–590 nm wavelength range.

A typical example of the results obtained during monitoring of tissue oxygenation in vivo before, during and after artificial vascular occlusion is shown in Fig. 5, where the dynamics of a decrease in oxygen saturation during occlusion and the return of tissue to its original condition after the restoration of blood supply are clearly visible. When performing this experiment on similar objects, the results were similar, but, naturally, not identical (due to different starting points, as well as random and systematic shifts along the time scale). Similar dynamics of oxygenation of biological tissues during occlusion was earlier experimentally observed and described by other research teams [31].

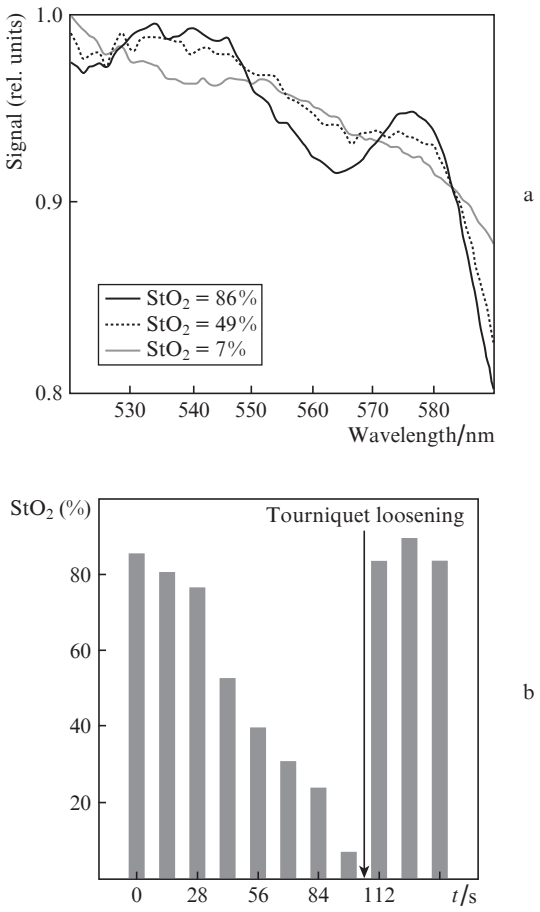

Figure 5. Examples of (a) normalised signals [right-hand side of Eqn (3)], obtained using the four-measurement method for monitoring artificial vascular occlusion in the ring finger, and (b) monitoring of the biotissue oxygenation before, during and after occlusion.

4. Conclusions

We have proposed an original method of four measurements for estimating the oxygen saturation of tissues. Statistical analysis of the accuracy of calculating the oxygenation of biological tissues using the developed method has shown that the error of the proposed method is smaller than the measurement error at the level of random noise of 5% and above. The method is implemented by fabricating a compact device with a reflective measurement geometry that allows probing tissues at a depth of 4 mm and automatically takes hardware parameters into account during experimental studies without prior calibration on a reference phantom. The results of testing the developed DOS system for monitoring the oxygen saturation of the tissue during artificial vascular occlusion agree with the data published earlier by other research teams. Thus, we can draw a conclusion about the viability of the proposed approach to the assessment of oxygenation of biotissues.

Acknowledgements. The work was supported by the Russian Foundation for Basic Research (Grant No. 16-32-60093 mol_a_dk). The authors are grateful to V.A. Vorob'ev and R.V. Belyaev for assembling the prototype DOS system, as well as to A.G. Orlova for discussing the results and helping to write the paper.

References

1. Cerussi A. et al. *Philos. Trans. A. Math. Phys. Eng. Sci.*, **369**, 4512 (2011).
2. Maslennikova A. et al. *J. Biophoton.*, **3**, 743 (2010).
3. Papazoglou E. et al. *Biomed. Instrum. Technol.*, **41**, 83 (2007).
4. Sujatha N. et al. *J. Appl. Spectrosc.*, **82**, 432 (2015).
5. Scheufler O. et al. *Plast. Reconstr. Surg.*, **113**, 141 (2004).
6. Whitaker I. et al. *J. Reconstr. Microsurg.*, **28**, 149 (2012).
7. Raleigh J. et al. *Radiat. Res.*, **151**, 580 (1999).
8. Ehling J. et al. *Thromb. Haemost.*, **109**, 375 (2013).
9. Durduran T. et al. *Rep. Prog. Phys.*, **73**, 076701 (2010).
10. Turchin I.V. *Phys. Usp.*, **59**, 487 (2016) [*Usp. Fiz. Nauk*, **186**, 550 (2016)].
11. Lee J. et al. *Physiol. Meas.*, **27**, 757 (2006).
12. Pham T. et al. *Rev. Sci. Instrum.*, **71**, 2500 (2000).
13. O'Sullivan T. et al. *J. Biomed. Opt.*, **17**, 071311 (2012).
14. Zhao H. et al. *Appl. Opt.*, **44**, 1905 (2005).
15. Kienle A. et al. *Appl. Opt.*, **35**, 2304 (1996).
16. Nichols M. et al. *Appl. Opt.*, **36**, 93 (1997).
17. Perekatova V. et al. *Biomed. Opt. Express.*, **7**, 3979 (2016).
18. Gill P. et al. *Practical Optimization* (London: Academic Press, 1981).
19. Contini D. et al. *Appl. Opt.*, **36**, 4587 (1997).
20. Kleshnin M. et al. *Proc. SPIE*, **10412**, 1041212 (2017).
21. Wang L., Wu H. *Biomedical Optics* (Hoboken: Wiley, 2007).
22. http://omlc.org/spectra/index.html.
23. Kleshnin M.S. et al. *Quantum Electron.*, **47**, 355 (2017) [*Kvantovaya Elektron.*, **47**, 355 (2017)].
24. Nocedal J., Wright S. *Numerical Optimization* (New York: Springer, 2006).
25. Tuchin V.V. *Tissue Optics: Light Scattering Methods and Instruments for Medical Diagnosis* (Bellingham, WA: SPIE Press, 2007).
26. Farrell T., Patterson M., Wilson B. *Med. Phys.*, **19**, 879 (1992).
27. Witte R., Witte J. *Statistics 10th Edition* (Hoboken: Wiley, 2013).
28. Rahman M., Govidarajulu Z. *J. Appl. Stat.*, **24**, 219 (1997).
29. Fay M., Proschan M. *Statistics Surveys*, **4**, 1 (2010).
30. Ogilvy C. et al. *J. Neurosurg.*, **84**, 785 (1996).
31. Casavola C. et al. *J. Biomed. Opt.*, **5**, 269 (2000).